09:39:31 OCA PAD INITIATION - PROJECT HEADER INFORMATION 09/09/88

Active

Project #: E-16-687 Cost share #: Rev #: 0
Center # : R6587-0A0 Center shr #: OCA file #:
Work type : RES
Contract#: 0389 Mod #: Document : PO
Prime #: Contract entity: GTRC

Subprojects ? : N
Main project #:

Project unit: AE Unit code: 02.010.110
Project director(s):
PRICE E W AE

Sponsor/division names: MORTON THIOKOL INC /
Sponsor/division codes: 212 / 032

Award period: 880701 to 900630 (performance) 900630 (reports)

Sponsor amount	New this change	Total to date
Contract value	130,000.00	130,000.00
Funded	65,000.00	65,000.00
Cost sharing amount		0.00

Does subcontracting plan apply ?: N

Title: STUDY OF THE OSCILLATORY INTERACTION OF SOLID PROPELLANT COMBUSTION...

PROJECT ADMINISTRATION DATA

OCA contact: William F. Brown 894-4820

Sponsor technical contact

DR. D. A. FLANIGAN
(801)625-4996
MORTON THIOKOL, INC.
P.O. BOX 9260
OGDEN, UT 84409

Sponsor issuing office

MR. R. W. SEARLE
(801)625-4988
MORTON THIOKOL, INC., AEROSPACE GRP.
P.O. BOX 9260
OGDEN, UT 84409

Security class (U,C,S,TS) : U ONR resident rep. is ACO (Y/N): N
Defense priority rating : NA NA supplemental sheet
Equipment title vests with: Sponsor X GIT

Administrative comments -
INITIATION OF E-16-687. FIXED PRICE P.O.

GEORGIA INSTITUTE OF TECHNOLOGY
OFFICE OF CONTRACT ADMINISTRATION

NOTICE OF PROJECT CLOSEOUT

SRC1

Closeout Notice Date 06/29/90

Project No. E-16-687 Center No. R6587-0A0

Project Director PRICE E W School/Lab AE

Sponsor MORTON THIOKOL INC/

Contract/Grant No. 0389 Contract Entity GTRC

Prime Contract No.

Title STUDY OF THE OSCILLATORY INTERACTION OF SOLID PROPELLANT COMBUSTION...

Effective Completion Date 890630 (Performance) 890630 (Reports)

Closeout Actions Required:	Y/N	Date Submitted
Final Invoice or Copy of Final Invoice	Y	
Final Report of Inventions and/or Subcontracts	N	
Government Property Inventory & Related Certificate	N	
Classified Material Certificate	N	
Release and Assignment	N	
Other	N	

Comments

Subproject Under Main Project No.

Continues Project No.

Distribution Required:

Project Director	Y
Administrative Network Representative	Y
GTRI Accounting/Grants and Contracts	Y
Procurement/Supply Services	Y
Research Property Managment	Y
Research Security Services	N
Reports Coordinator (OCA)	Y
GTRC	Y
Project File	Y
Other	N
	N

GEORGIA INSTITUTE OF TECHNOLOGY
ATLANTA, GEORGIA 30332

SCHOOL OF
AEROSPACE ENGINEERING

404-894-3000

DANIEL GUGGENHEIM SCHOOL
OF AERONAUTICS

17 February 1989

TO: R. Kruse, Morton Thiokol, Inc., Huntsville

FROM: E. W. Price

SUBJECT: Progress on Contract No. 0389

1. Progress on the subject contract is in the following areas:

   a. Analytical - computational modeling of the leading edge of diffusion flames
   b. Role of leading edge flame detachment in controlling mean burning rate and oscillatory combustion
   c. Determination of "smooth band width" (experimental input to the Deur-Price model for dynamic response)

These topics will be described below, with further detail on item a) in the attachment.

2. Leading edge flames:

The microsopic flame that governs combustion behavior of AP propellants consists of areas of AP self deflagration near the AP surface, and oxidizer-fuel flames in the mixing fans that originate along the oxidizer-fuel contact lines on the propellant surface. The O-F flames include outer sections that can be modeled by classical diffusion flame models (in which reaction kinetics are not very important), and inner "leading edge" portions in which kinetics are important and analytical models are deficient. Unlike most diffusion flame problems, in the propellant O-F flamelets the leading edge part is the most

important part. Under many conditions, most of the O-F reaction occurs in this kinetically controlled region, which is the main source of heat to the burning surface. The leading edge flame controls burning rate, dynamic response, pressure dependence of rate, particle size effects and low pressure deflagration limits. It has been only crudely modeled in the past, and no direct measurements of its behavior have been possible (because the flame is too small to see). We have been working for some time on development of an analytical-computational model that would permit us to study the characteristics of these diffusion flamelets. The practical goal is to provide a more sound basis for predicting or controlling propellant combustion behavior. The short-term goal is to be able to calculate the diffusion-reaction field and the character of the leading edge flame, using computation methods that are not prohibitively expensive. The approach to date has been to use a two-dimensional laminar mixing field, time dependent (Navier Stokes) flow, and a reaction scheme for methane and air as the fuel and oxidizer. The upstream boundary conditions at present are chosen to match a companion gas burner experiment (separately funded study) so as to permit experimental evaluation of computational results. Adaptation to propellant-like conditions will be made after more is learned about the behavior of leading edge flames. Progress to date is summarized in Attachment A, which was prepared by Mr. Kuldeep Prasad from his Ph.D. thesis research.

3. Leading edge flame detachment:

Analytical models of propellant combustion that take into account the role of leading edge flames (LEFs) picture the flame as standing off from the surface by some distance that is dependent on pressure. However, the nature of the mixing field above the surface is such that the leading edge flame can occur only over a certain range of stand-off distances, which are dependent on oxidizer particle size and pressure. When size or pressure are reduced too much, the LEF "goes out", leading to quench of burning or transition to a different mode of burning rate control. This transition is not considered in existing theoretical models of propellant combustion, but is believed (by this author) to be qualitatively important. Its effect was demonstrated in the case of burning rate of bimodal AP

propellants by results in Fig. 1, which show a transition region in the burning rate vs pressure curves in the pressure range where LEF detachment is occurring on the fine AP particles (thereby reducing the fine particle effect on rate at low pressure). Such an effect is expected to be important to more conventional particle size distributions as well, but doesn't lead to a sharp transition region (bimodal AP was chosen because it concentrates the effect in a narrow pressure range that is identifiable with the LEF detachment mechanism). The LEF detachment process is believed to be important also to oscillatory combustion; particles that are burning near the threshold for LEF detachment would be expected to extinguish and recover during a cycle of pressure oscillation, producing a disproportionately large contribution to the collective response of all particles. This proposition has been posed earlier in this project in the form of a research proposal that would require preparation of special propellants, and a T-Burner testing program. We have continued to explore means to carry out these tasks, and now have some prospect that the Office of Naval Research will fund the study to be done jointly by Georgia Tech and the U. S. Naval Weapons Center. Morton Thiokol support has provided a thread of continuity of effort on the important issue of LEF detachment that has saved the issue from "extinction", and will be acknowledged in any reports on the subject.

The importance of LEF detachment emerged over the last six months in the context of another project. As a chapter in a book on combustion instability, the subject of L^* instability was chosen as a "beginners" introduction, because L^* instability was considered to be a tractable problem with theory in good shape. A set of 20-year-old test data was chosen to show calculation procedure, experimental trends, and comparison with theory. The trend of experimental results did not conform to theory, an outcome that is now attributed in part of "anomalous" behavior of the bimodal AP propellant. A careful look at the data suggests that the combustion response is very nonlinear, a property we would expect if LEF detachment were a major factor. We are continuing the study of L^* burner results, data for which are available for several bimodal and unimodal propellants. This work is acquainting the student (Mr. Chris Beiter) with the

concepts of combustion instability, and at the same time will probably bring forth a convincing demonstration of the importance of LEF detachment.

4. Smooth band width

In our studies of combustion zone microstructure, we have observed that the surface of AP particles on the burning surface includes a central area that is "self deflagrating", and a peripheral area that is subliming, with a distinctive smoothness of the surface (inhibited from self deflagrating by lateral subsurface flow of heat to the endothermic binder). In the Deur-Price model for dynamic response of combustion, the smooth band is treated as the portion of the oxidizer vapor that is consumed in the LEF. We are collecting and reviewing results from quench burns of AP-binder-AP sandwiches to determine how the width of smooth bands depends on pressure and binder thickness. This data will be used by Dr. Duer in his continuing studies at Thiokol.

EWP/ed
prprpt.T14
2/89

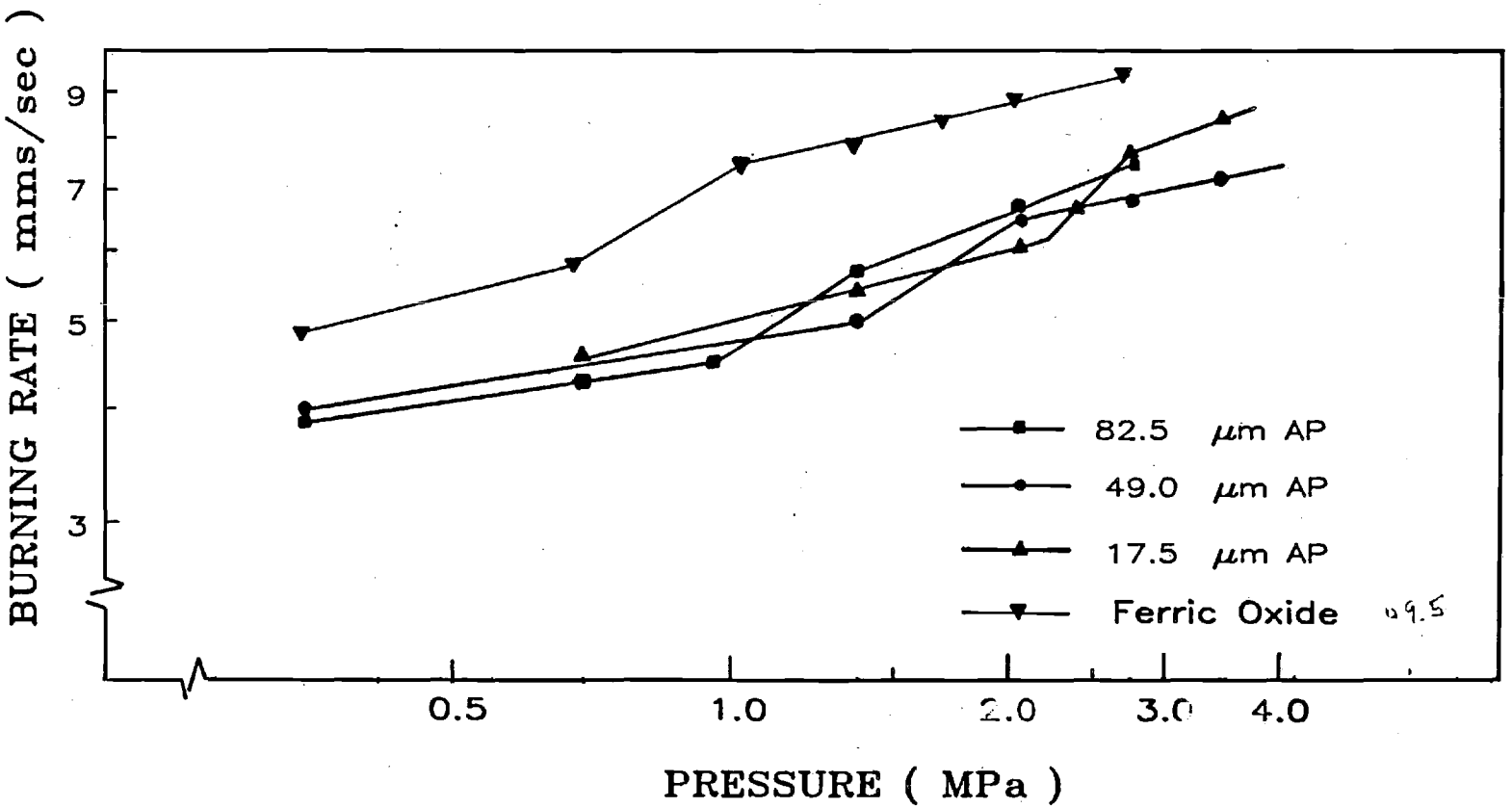
BURNING RATE (mms/sec)
9
7
5
3
0.5
1.0
2.0
3.0
4.0
PRESSURE (MPa)
82.5 μm AP
49.0 μm AP
17.5 μm AP
Ferric Oxide

Numerical Simulation of multi-component chemically reacting fluid flow

Introduction:

The current research has been directed towards gaining a detailed understanding of the complex flow field and the flame structure obtained when a mixing flow undergoes chemical reactions. A numerical model is being developed for describing a general, two dimensional subsonic flow through a burner as shown in figure 1. The program has been constructed to consider the viscous effects in a mixing layer, the multi-component diffusion and convection of important species, the finite rate reaction of these species and the resulting interaction between the fluid mechanics and the chemistry. The problem chosen though geometrically simple still retains the fluid mechanical and chemical complexities that are under consideration.

Finite difference formulation

Fluid flow

The two dimensional Navier-Stokes, energy and species continuity equations along with the rate expressions completely describe the flow through a burner. A modified MacCormack finite difference scheme is used to discretize the governing equations. The scheme is second order accurate in space and time.

The governing equations require boundary conditions along all four boundaries. For the problem being considered, the inflow boundary is always subsonic. Characteristic theory allows three quantities to be specified at the subsonic inflow boundary At the air inflow boundary the total density and the total momentum in both directions is specified. Symmetry boundary condition is specified at the burner centre-line. At the subsonic outflow boundary characteristic theory allows the specification of only one quantity, and only the outflow static pressure is specified. No slip boundary condition(u=0,v=0) are used to specify velocity compoenents along

the solid surfaces that occur in the phyysical domain. The walls may be assumed as non adiabatic or non catalytic under certain situations.

Diffusion Velocities

Computaion of diffusion velocities in a multi species flow such as diffusion flames is of paramount interest. In general the diffusion equations are singular matrix equations, so not only is an expensive matrix inversion required, but an additional constraint is necessary to extract a particular solution. Because the straight forward inversion to find the diffusion velocities requires on the order of N_s cube operations, a more efficient perturbation analysis is employed which requires of the order N_s squared operations. (N_s is the no. of species.)

A Leonnard-Jones potential is computed for each species. Non-equilibrium kinetic theory is used to obtain the diffusion coefficients, thermal conductivity and viscousity.

Chemical Reactions

This section addresses the need for a fast batch chemistry solver to perform the kinetics part of a split operator formulation in a reacting flow. Seeking computationally efficient methods for approximately solving the stiff, strongly coupled non-linear ODE's requires that the actual source of difficulty be recognized, that is, whether specific computaional problem arise from the physics of the system or from an inappropriate choice of numerical methods.

In an evolving combustion problem three distinct physical and chemical regimes, commonly denoted as induction, heat release and equilibration, are apparent. The induction regime is the period immediately following some form of homogenous bulk ignition. During the induction period concentrations of reactant precursors and intermediate chain carriers increase by many orders of magnitude, from very small concentrations to values sufficient to initiate exothermic reactions. During the induction period the coupling with the energy equation is weak, so that an essentially isothermal reaction is obtained. At the end of the induction period, observable ignition occurs, as exhibited by an exponentially

increasing temperature and accompanying rapid depletion of reactant concentrations.

The induction period ends and the heat release period begins, when sharply defined changes in temperature and molar concentrations occur. In this regime the full chemical mechanism is active, with very strong temperature coupling through the enthalpy conservation equation.

The equilibration regime is characterized by the monotonic, asymptotic approach of all species concentrations and of the temperature toward their chemical equilibrium values. The equilibration process does not have a clearly defined termination, because of the asymptotic nature of the approach to the equilibrium state. An efficient Gibb's function minimization scheme is used to define the equilibrium state. The end of equilibration period can then be defined as the time at which the values of all thermochemical variables are within 1 percent of their equilibrium values.

Each of these physical regimes impose it's own unique computaional difficulty on the integration algorithm. Any physical system which shows a strong directional drive towards some form of equilibrium state is described by stiff ODE's. Typically the exact solution of stiff ODE's exhibit the general appearance of decaying exponential functions.

The equilibration regime is characterized by the asymptotic approach of all chemical species and temperature towards their equilibrium states. Therefore, using the above definitions of stiffness, we can classify the equilibration regime as stiff. During induction, however, many species and the temperature have positive time constants, which indicate unstable ODE's. The induction regime is therefore nonstiff. Since the heat-release regime is not clearly stiff, it must be regarded as nonstiff as well.

Some of the choices that have to be made in selecting the best implicit methods are whether to converge the corrector equations by successive substitution {Jacobi, Gauss-Seidel, or Jacobi-Newton iteration}, or by simultaneous substitution {Newton-Raphson iteration}, and if by Newton-Raphson iteration, whether to choose pivotal Gauss elimination, LU-decompostion or Hessenberg

decomposition to carry out the work intensive matrix operations required. All these choices are interdependent and highly problem-dependent, so that a single, best, all-purpose computational method for all problems does not yet exist.

Kinetics

Test runs are presently being made for hydrocarbon flames(methane, propane). One step reactions to account for the chemistry are certainly inadequate in describing the details of the interaction between fluid mechanics and chemistry. The set of elementary reactions must model the chemistry for all fuel/oxidizer ratios, particularly important while modeling diffusion flames. The reaction set must be self igniting (i.e. should not require addition of radicals to initiate chemical reactions).

In general the larger the set of elementary reactions larger is the computational effort spent per time step in integrating the rate equations. A set of 4 reactions with 8 species was chosen for modelling methane chemistry. The scheme performed well for lean fuel cases but was not satisfactory for fuel rich mixtures. It was found that addition of hydrogen(H) atoms were necessary to initiate chemical reactions. The scheme also required an initial concentration of hydrogen(H_2) molecule. The time step that we were required to use to integrate the chemistry was extremely small and this was resulting in extremely large computational costs. We are now working on a more expensive elementary reaction scheme that involved 59 reactions and 20 species. We found that this scheme allowed us to march at a much larger time step. Thus the total computational effort in this case was found to be smaller than the case of 4 reactions.

Concluding Remarks

A computer program is being developed to model the details of a subsonic, chemically reacting and spatially developing hydrocarbon-air mixing layers. The program solves the general form of the two-dimensional Navier-Stokes equations along with a set of species continuity equations. Diffusive transport of the species is

described using a multicomponent perturbation diffusion model, and chemical reaction is described using an 59 reaction finite-rate model for the methane-air system.

Burner Geometry

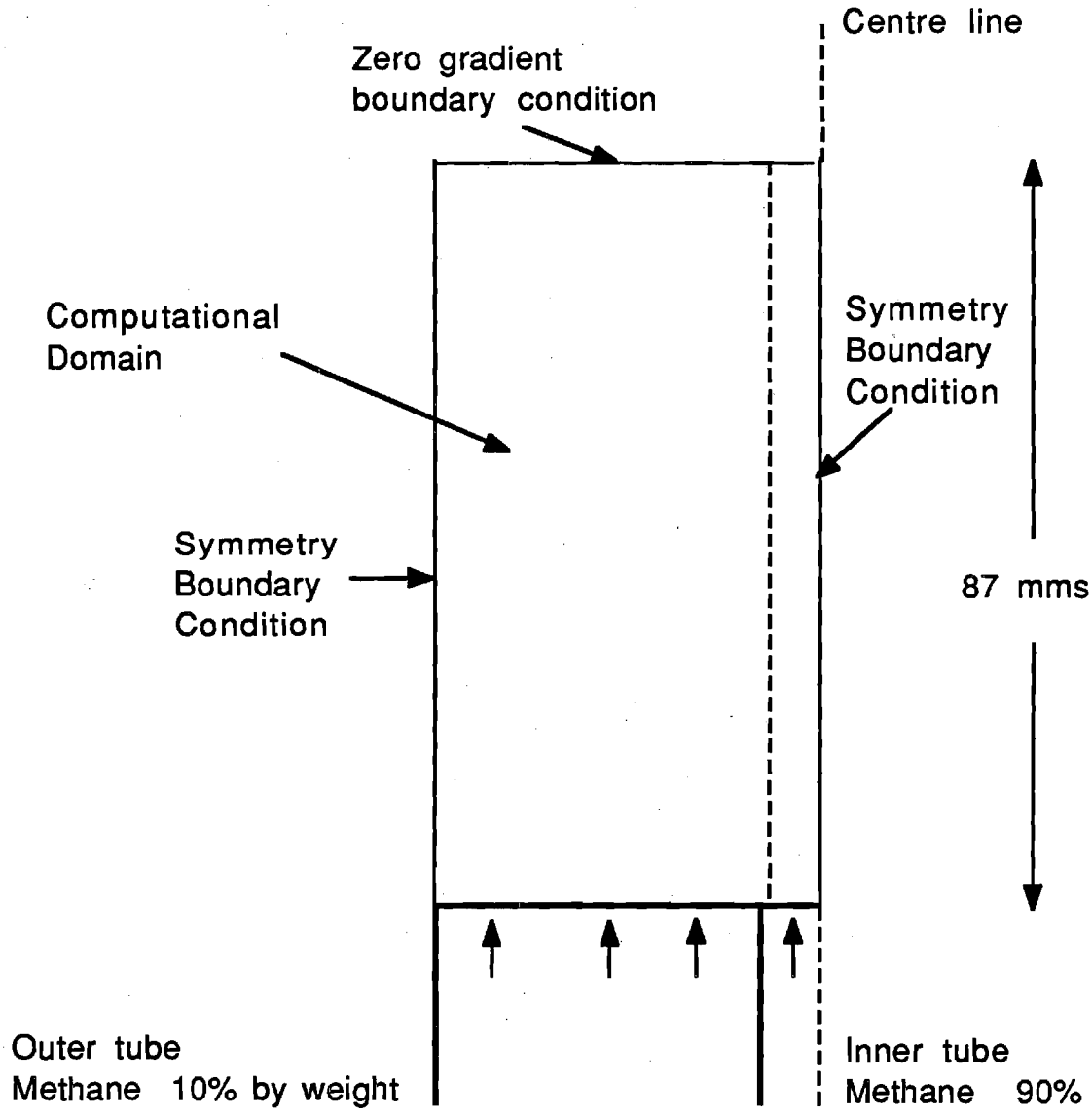

Outer tube
Methane 10% by weight
Oxygen 90% by weight
Velocity 40 cms/sec
Pressure 1 atm.
Temperature 298.15 K
Half thickness 8.825 mms..

Inner tube
Methane 90% by weight
Oxygen 10% by weight
Velocity 20 cms/sec
Pressure 1 atm.
Temperature 298.15 K
Half thickness 3.175 mms..

School of Aerospace Engineering

Georgia Institute of Technology
Atlanta, Georgia 30332-0150
404·894·3000
Fax: 404·894·2760

14 December 1989

TO: R. B. Kruse, Thiokol, Inc.

FROM: E. W. Price

SUBJECT: Progress on Contract #0389, 1 Aug. - 1 Dec. 1989

1. During the above period progress was made on three topics.

a) The analytical-computational study of the two-dimensional model of diffusion flame progressed to the point where supercomputer time is the principal limitation on progress. Status is described in detail in Attachment #2.

b) Experimental determination of "smooth band width" vs binder thickness and pressure is being determined for AP-binder sandwiches. This is input data needed for the Deur-Price model of dynamic combustion response of AP composite propellants to pressure oscillation (currently being developed at Thiokol Huntsville by J. M. Deur). This study is explained in Attachment #1.

c) An experimental study of oscillatory combustion response of bimodal propellants, originally proposed for this project, has been partially carried out with the help of ONR funding and facilities support of the Naval Weapons Center. A preliminary report on results will be provided in the next quarterly report to Thiokol, because the study pertains to a possibly important extension of the Deur-Price combustion response model to encompass a flame behavior referred to as "leading edge flame detachment".

d) A study started some years ago (and abandoned) has been renewed, and will hopefully provide fundamental input data for parts b) and c) above. Combustion studies are being made on AP-Binder-AP sandwiches in which the binder lamina has fine AP powder in various concentrations and with various particle sizes. This is a way to study and understand the still mysterious combustion behavior of propellants with widely separated bimodal AP size distributions, to study flamelet interactions between adjoining particles of unlike size, and to study leading edge flame detachment. One student has chosen this investigation for his Ph.D. thesis topic.

Attachment #1

"SMOOTH BANDS"

Christos Markou and E. W. Price

When AP-hydrocarbon binder propellants burn, the surfaces of the AP particles exhibit a singular feature referred to as a "smooth band" around the periphery (Fig. 1). This portion of the decomposing surface is believed to decompose by endothermic dissociative sublimation, whereas the rest of the surface is believed to decompose by an exothermic process in a surface froth and near-surface monopropellant flame. The significance of this behavior is intricately linked with the structure of the O-F flamelets above the surface and the multi-dimensional heat flow from those flamelets to the surface and in the heterogeneous condensed phase. These features of the combustion process have been clarified by studies of combustion of edge-burning AP-binder laminates, which exhibit the same features under less complex conditions (Fig. 2 and Ref. 1). On the basis of the microstructure of the combustion zone revealed by these studies, Deur developed an analytical-computational model of the dynamic response to imposed pressure oscillations (Ref. 2). Implementation of this model requires the width of the smooth band as an experimental input.

In past studies of laminate burning, no effort was made to determine smooth band width as a function of relevant variables (which are primarily mean pressure and binder lamina thickness. To obtain this data, a series of tests is being conducted [at different pressures] using sandwiches with "tapered" binder laminae; on the burning edge the thickness goes from about 100 μm on one end to near-zero thickness at the other end). Samples are burned on the "tapered" edge and quenched by rapid depressurization, and then examined by scanning electron microscopy. The samples used in this study are made from AP laminae cleaved from large single crystals of AP in order to obtain uniform smooth bands (previous tests have generally used AP laminae formed by dry pressing granular AP). At present the test samples are all fabricated and most of the interrupted burning tests are completed.

References

1. Price, E. W., Sambamurthi, J. K., Sigman, R. K., and Panyam, R. R., "Combustion of Ammonium Perchlorate-Polymer Sandwiches," Combustion and Flame, Vol. 63, 1986, pp. 381-413.

2. Deur, J. M., "A Surface-Coupled Flamelet Approach to Dynamic Response in Heterogeneous Propellant Combustion," Ph.D. Thesis, Georgia Institute of Technology, Atlanta, GA, Sept. 1988.

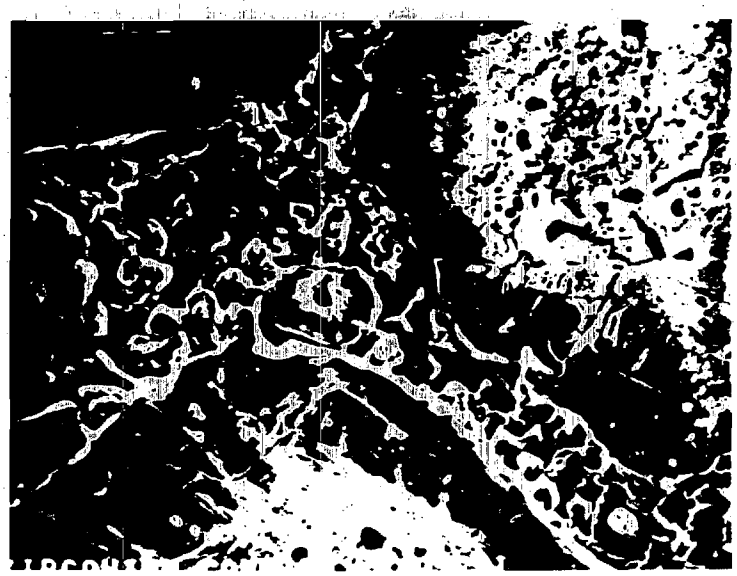

Fig. 1 Surface of propellant sample quenched by rapid depressurization, showing a "smooth band" around the periphery of AP particle surfaces.

Fig. 2 Surface of AP-PBAN-AP sandwich quenched by rapid depressurization, showing smooth band on AP surface along AP-Binder interface line.

Attachment #2

NUMERICAL MODELING OF REACTIVE FLOWS THROUGH TWO-DIMENSIONAL BURNERS

K. Prasad and E. W. Price

ABSTRACT

This study deals with a fundamental numerical investigation of chemically reacting fluid flows through 2-D burners. We make use of a detailed set of finite chemical kinetic rate equations to numerically simulate a laminar diffusion flame. The code has been constructed to consider the viscous effects in a mixing layer, heat conduction, the multi-component diffusion and convection of important species, the finite rate reactions of these species, and the resulting interactions between the fluid mechanics and the chemistry.

INTRODUCTION

One of the most commonly obtained flame structures in most practical combustion devices are the diffusion flames. These flames are characterized by the presence of a narrow reaction zone stabilized between two co-flowing jets of fuel and oxidizer. These flames are limited chiefly by the diffusion process between the fuel and the oxidizer (Ref. 1). The diffusion flame, however, does not extend all the way up to the burner surface, but in fact originates from a region where the reactions are limited by the kinetics of the fuel and the oxidizer. This numerical study is aimed at obtaining a more detailed understanding of the leading edge of the diffusion flame.

Obtaining an accurate structure of the diffusion flame is crucial while modeling combustion instability. In general, the ability to predict the coupled effects of complex transport phenomena with detailed kinetics is critical in predicting flammability limits. A detailed understanding of those factors that affect flame extinction is important in improving engine efficiency.

In the current work, a numerical model was developed for describing a general two-dimensional chemically reacting fluid flow. A computer program was constructed that numerically solves the governing equations resulting from the

model. The program uses a fractional step coupling approach to couple the fluid dynamics with the rate terms (Ref. 2). Momentum, heat, and mass diffusion are described by laws based on kinetic theory (Ref. 3); chemistry is defined by a finite rate scheme; and a real gas thermodynamic model is employed. Details of these models are given in the following sections.

ANALYSIS

GOVERNING EQUATIONS

The two-dimensional, Navier-Stokes, energy, and species continuity equations governing multiple species undergoing chemical reactions are given in index notation by (Ref. 4):

Overall Continuity Equation:

$$\frac{\partial \rho}{\partial t} + \frac{\partial (\rho u_i)}{\partial x_i} = 0 \qquad i, j = 1 \ldots 2 \tag{1}$$

Conservation of Momentum:

$$\frac{\partial (\rho u_i)}{\partial t} + \frac{\partial (\rho u_i u_j)}{\partial x_j} = \frac{\partial \tau_{ij}}{\partial x_j} + \sum_{k=1}^{N} \rho_k f_{i,k} \tag{2}$$

Conservation of Energy:

$$\frac{\partial (\rho e_t)}{\partial t} + \frac{\partial (\rho e_t u_i)}{\partial x_i} = - \frac{\partial q_i}{\partial x_i} + \frac{\partial (\tau_{ij} u_j)}{\partial x_i} + \sum_{k=1}^{N} \rho_k \, (u_i + U_{i,k}) \, f_{i,k} \tag{3}$$

Species Conservation Equation:

$$\frac{\partial \rho_k}{\partial t} + \frac{\partial (\rho_k u_i)}{\partial x_i} = - \frac{\partial (\rho_k U_{i,k})}{\partial x_i} + \dot{w}_k \qquad k = 1 \ldots N$$

$$\sum_{k=1}^{N} \rho_k = \rho \; ; \quad \sum_{k=1}^{N} \rho_k u_{i,k} = \rho u_i \; ; \quad \sum_{k=1}^{N} \rho_k U_{i,k} = 0 \tag{4}$$

where

$$\tau_{ij} = \left(-p + (\kappa - \frac{2}{3}\mu) \frac{\partial u_i}{\partial x_i} \right) \delta_{ij} + \mu \left(\frac{\partial u_i}{\partial x_j} + \frac{\partial u_j}{\partial x_i} \right) \tag{5}$$

$$q_i = \lambda \frac{\partial T}{\partial x_i} + \sum_{k=1}^{N} h_k \rho_k U_{i,k} + RT \sum_{k=1}^{N} \sum_{i=1}^{N} \frac{\rho_i D_{T,k}}{W_k D_{i,k}} + q_R \tag{6}$$

$$\rho e_t = \sum_{k=1}^{N} \rho_k h_k - p + \frac{\rho}{2} (u_i u_i) \tag{7}$$

$$h_k = h^o_{298} + \int_{T_o}^{T} C_{p_k} \, dT \tag{8}$$

$$p = R_o T \sum_{k=1}^{N} \frac{\rho_k}{W_k} \tag{9}$$

The diffusion velocities are found by solving

$$\frac{\partial X_k}{\partial x_i} = \sum_{j=1}^{N} \left(\frac{X_k X_j}{D_{kj}} (U_{i,j} - U_{i,k}) \right) + \frac{(Y_k - X_k)}{p} \frac{\partial p}{\partial x_i} + \frac{\rho}{p} \sum_{j=1}^{N} Y_k Y_j (f_{i,k} - f_{i,j})$$

$$+ \sum_{j=1}^{N} \left[\left(\frac{X_k X_j}{\rho D_{kj}} \right) \left(\frac{D_{T,j}}{Y_j} - \frac{D_{T,k}}{Y_k} \right) \right] \frac{\partial T}{T \partial x_i} \qquad k = 1 \ldots N \tag{10}$$

Note that if there are N chemical species then only N-1 species conservation equations are solved. The final species density is found by conservation of mass since

$$\sum_{k=1}^{N} \rho_k = \rho \tag{11}$$

The values of the various diffusion coefficients, such as viscosity, thermal conductivity, and the binary diffusion coefficients are obtained from a rigorous treatment of kinetic theory (Ref. 3).

CHEMISTRY MODEL

In the present model, the finite rate reaction of gaseous methane fuel and air is of concern. The reactions are modeled by a 15 species, 42 reaction model described in Table I.

The rate of production of each species is obtained by using the phenomonological expression of chemical kinetics

$$\dot{w}_k = \sum_{\ell=1}^{M} \left(\nu''_{k,\ell} - \nu'_{k,\ell} \right) \left[k_{f,\ell} \prod_{L=1}^{N} (C_i)^{\nu'_{i,\ell}} - k_{b,\ell} \prod_{L=1}^{N} (C_i)^{\nu''_{i,\ell}} \right] \quad k = 1 \ldots N \quad (12)$$

The forward rate of each reaction ℓ is given by the Arrhenius law

$$k_{f,\ell} = A_\ell T^{n_\ell} \exp\left(- \frac{E_\ell}{RT} \right) \qquad \ell = 1 \ldots M \quad (13)$$

Values of A, E, and n are also given in Table I (Ref. 9). Knowing the forward reaction rate, we determine the reverse reaction rate by using the equilibrium constant determined in the next section.

$$k_{b,\ell} = \frac{k_{f,\ell}}{K_p} \qquad \ell = 1 \ldots M \quad (14)$$

THERMODYNAMIC MODEL

To calculate the required thermodynamic quantities, the specific heat for each species is defined by a fourth order polynomial in temperature

$$C_{p,k} = \sum_{\ell=1}^{5} a_{\ell,k} T^{\ell-1} \qquad k = 1 \ldots N \quad (15)$$

The enthalpy of each species is then found from Eq. (8). To determine the equilibrium constant for each elementary chemical reaction the Gibbs free energy of each species is found by using

$$G^o = H^o - TS^o \tag{16}$$

For the general chemical reaction $\sum_{k=1}^{N} \nu_k A_k = 0$, the standard change of free energy due to this reaction is given by $\Delta G^o = - \sum_{k=1}^{N} \nu_k (G^o)_k$

The equilibrium constant K_p for any general chemical reaction is then defined by using

$$R \ln K_p = - \frac{\Delta G^o}{T} \tag{17}$$

DISCRETIZATION OF THE GOVERNING EQUATION

The complete set of Navier-Stokes equation can be expressed as

$$\frac{\partial U}{\partial t} + \frac{\partial F}{\partial x} + \frac{\partial G}{\partial y} = H \tag{18}$$

where U contains the accumulation terms, F and G contain the convective and diffusive terms in the two coordinate directions, and H contains the source terms.

The governing equations (1-4) are written in the physical domain (x,y), and must be transformed to an appropriate computational domain (ξ,η) for solution. The physical domain is highly compressed in both the x,y directions in the region where fuel and oxidizer mix. The grid, however, is required to be uniform in the computational domain to most readily maintain a required order of accuracy.

In the computational domain, equations (1-4) can be written as

$$\frac{\partial \bar{U}}{\partial t} + \frac{\partial \bar{F}}{\partial \xi} + \frac{\partial \bar{G}}{\partial y} = \bar{H}$$

where

$$\bar{U} = \frac{U}{J} \; ; \; \bar{F} = \frac{F}{J} \xi_x \; ; \; \bar{G} = \frac{G}{J} \eta_y ; \; \bar{H} = \frac{H}{J} \qquad (19)$$

Here ξ_x, η_y are the transformation metrics, and J is the Jacobian of the transformation.

One of the major problems associated with computations of chemically reacting fluid flows is the presence of time scale associated with the rate term that may be the same as, or very different from, the fluid dynamic time scale. Such a range of time scales referred to as stiffness can create major computational difficulties. If the chemical time scale is much smaller than the time scale of interest, then, of course, an equilibrium chemistry model can be used in place of the finite rate model. However, for many problems the chemical time scale can vary significantly throughout the region of interest. Since this variation is not known a priori, a computational method must be able to handle a wide range of time scales.

We therefore resorted to a fractional step approach (Ref. 2, 5), in which the individual processes are solved independently and the changes resulting from the separate partial calculations are coupled together. Since the reaction rate term is responsible for the stiffness in the problem, it was decoupled from the fluid dynamic equations. This allowed the time step integrating procedure to march at the fluid dynamic time step, which may be orders of magnitude larger than the smallest chemical time scale.

The fluid dynamic equations are advanced in time using an unsplit form of the MacCormack predictor corrector finite difference scheme (Ref. 6) as shown below.

$$(\Delta \bar{U})^{\overline{n+1}}_{i,j} = - \Delta t \, (\bar{F}^{n}_{i+1,j} - \bar{F}^{n}_{i,j}) - \Delta t \, (\bar{G}^{n}_{i,j+1} - \bar{G}^{n}_{i,j})$$

$$\overline{\bar{U}}^{n+1}_{i,j} = \bar{U}^{n}_{i,j} + \overline{\Delta\bar{U}}^{n+1}$$

$$(\Delta\bar{U})^{n+1}_{i,j} = - \Delta t \, (\overline{\bar{F}}^{n+1}_{i,j} - \overline{\bar{F}}^{n+1}_{i-1,j}) - \Delta t \, (\overline{\bar{G}}^{n+1}_{i,j} - \overline{\bar{G}}^{n+1}_{i,j-1})$$

$$\bar{U}^{n+1}_{i,j} = \bar{U}^{n}_{i,j} + 0.5^{*} \, (\Delta\bar{U}^{n+1}_{i,j} + \overline{\Delta\bar{U}}^{n+1}_{i,j}) \qquad (20)$$

Once the various fluid quantities such as density, momentum, total energy, and species densities have been obtained at the new time level, the temperature and pressure are obtained by an iterative solution of Eq. (7) - (9).

INTEGRATION OF THE KINETIC RATE EQUATIONS

This section describes an algorithm for the fast automatic integration of the kinetic rate equations given by

$$\frac{\partial \rho_k}{\partial t} = \dot{w}_k \, (T, \, \rho_i) \quad k = 1 \ldots N \qquad (21)$$

The two part predictor corrector algorithm, based on an exponentially fitted trapezoidal rule (Ref. 7, 8), includes filtering of ill-posed initial conditions, automatic step size selection, and automatic selection of Newton-Jacobi or Newton iterative convergence to achieve maximum computational efficiency while observing a prescribed error of tolerance.

The algorithm makes use of the fact that the rate equations are mathematically non-stiff during the induction and heat release regime. In this regime, small step sizes are required regardless of the choice of the integration algorithm. Here the computationally inexpensive Jacobi-Newton point iterative technique was used. During the equilibration regime, the governing equations are stiff and the large time steps admitted by accuracy requirements are too large for convergence for point iterative techniques. We therefore used the full Newton iteration to converge the governing equations which involves the evalua-

tion of the Jacobian matrix, and the solution of a matrix system of dimension N by N, where N is the number of species.

EVALUATION OF THE DIFFUSION VELOCITIES

The exact diffusion equation (10) is solved to obtain the diffusion velocities of the species in the x and y direction. It should be noted that for a system containing N species, the system of equations defined by Eq. (10) are not linearly independent. Here we make use of the fact that the diffusion velocities introduce no net momentum to the fluid flow. The equation

$$\sum_{k=1}^{N} \rho_k U_{i,k} = 0 \tag{22}$$

is used as a constraint equation and a least squares approach is used to obtain the diffusion velocities in the x and y directions.

BOUNDARY AND INITIAL CONDITIONS

The governing equations, being parabolic in time, require boundary conditions along all four boundaries. For the present problem, the inflow boundary is always subsonic. Theory of characteristics allows us to prescribe three conditions at the inlet surface. The density and the mass flux in the x and y directions are prescribed at the inlet.

Symmetric boundary conditions are used at the center line of the two-dimensional burner. All normal gradients are required to vanish along the upper boundary. Finally, no slip boundary condition was used at all solid surfaces in the computational domain. Additionally, along these solid boundaries, adiabatic conditions are assumed, the boundary layer assumption on pressure is chosen, and the walls are assumed to be non-catalytic.

The finite differece formulation advances the solution of the governing differential equations to the desired time level starting from a prescribed set of initial conditions. The better the initial conditions, the faster is the rate

of convergence to the steady state solution.

RESULTS AND DISCUSSION

One of the major concerns during the course of this work has been the large computational costs associated with time simulation of reactive flows through two-dimensional burners. In order to reduce computational costs during the code development phase, several smaller problems were tested.

Using the numerical model and the finite difference scheme given in the previous sections, an unsteady state, one-dimensional flame propagation model was formulated for predicting the characteristics of premixed methane-air flames. The test condition used a lean CH_4/O_2 flame (9.5% CH_4, 90.5% O_2) burning at 40 torr. The fresh gas stream velocity was 67 cm/sec. The simulation was performed on a set of 30 equally spaced grid points. The total CPU cost for this problem was approximately 720 seconds on the CRAY-YMP class of computers. A detailed experimental study for such a configuration was done by Peeters and Mahnen (Ref. 10). Figure 1 provides a comparison between numerical predictions and experimental observations of the temperature profile above the burner surface. Figures 2, 3, 4, 5, 6, 7, 8 compare the predicted and experimental mole fractions of reactants, products, and other intermediate species. Figures 9 and 10 show the trend of total density (kg/m^3) and pressure above the burner surface.

The second test was aimed at integrating the kinetic rate equations in the absence of the fluid dynamic effects. A volume of fluid (10% CH_4, 20% O_2, 70% N_2) was raised to a temperature above the ignition temperature. The pressure was kept constant at 1 atm. Figures 11 and 12 show the changes in temperature and concentration of major species as a function of time. The third test was aimed at obtaining the flow field, when two parallel streams of gases flow through a 2-D burner. The test was performed in the absence of chemical reactions. The half thickness of the inner and outer tube were 4.35 mm and 30.0 mm respectively. The composition of the gases through the inner tube was 23.2% CH_4 and 76.8% N_2. The composition of the gases through the outer tube was 23.2% O_2 and 76.8% N_2. Fresh gases flowed at a velocity of 40 cm/sec through both the inner and outer tube. Figures 13 and 14 show the concentration profiles obtained at different heights above the burner surface.

Results on 2-D reactive flows have been severely restricted by the large computational costs associated with the problem. Present efforts have been directed toward providing good initial conditions for the time marching problem. It is expected that better initial conditions would result in faster rate of convergence toward the steady state solution. We are also attempting use of H_2 as fuel, instead of CH_4. Preliminary results indicate that 2-D reactive flow problems with hydrogen as fuel are computationally much less expensive.

REFERENCES

1. Price, E. W., Sambamurthi, J. K., Sigman, R. K., Panyam, R. R., "Combustion of Ammonium Perchlorate-Polymer Sandwiches," Combustion and Flame, Vol. 63, 1986, pp. 381-413.

2. Yanenko, N. N., The Method of Fractional Steps, Springer-Verlag, New York, 1971.

3. Hirschfelder, J. O., Curtiss, C. F., and Bird, R. B., Molecular Theory of Gases and Liquids, John Wiley and Sons, Inc., New York, 1954.

4. Kuo, K. K., Principles of Combustion, John Wiley, New York, 1986.

5. Oran, E. S., and Boris, J. P., Numerical Simulation of Reactive Flows, Elsevier Publication, 1987.

6. MacCormack, R. W., and Baldwin, B. S., "A Numerical Method for Solving the Navier-Stokes Equations with Application to Shock Boundary Layer Interactions," AIAA Paper 75-1, 1975.

7. Brandon, D. M., Jr., "A New Single Step Implicit Integration Algorithm with A-Stability and Improved Accuracy," Simulation, 23, 17, 1974.

8. Radhakrishnan, K, and Pratt, D. T., "Fast Algorithm for Calculating Chemical Kinetics in Turbulent Reacting Flow," Combustion Science and Technology, Vol. 58, 1988, pp. 155-176.

9. Gardiner, W. C., Jr., Combustion Chemistry, Springer-Verlag, New York, 1984.

10. Peeters, J., and Mahnen, G., "Reaction mechanism and Rate Constants of Elementary Steps in Methane-Oxygen Flames," Fourteenth Symposium (International) on Combustion, 1973, pp. 133-146.

Results on 2-D reactive flows have been severely restricted by the large computational costs associated with the problem. Present efforts have been directed toward providing good initial conditions for the time marching problem. It is expected that better initial conditions would result in faster rate of convergence toward the steady state solution. We are also attempting use of H_2 as fuel, instead of CH_4. Preliminary results indicate that 2-D reactive flow problems with hydrogen as fuel are computationally much less expensive.

REFERENCES

1. Price, E. W., Sambamurthi, J. K., Sigman, R. K., Panyam, R. R., "Combustion of Ammonium Perchlorate-Polymer Sandwiches," Combustion and Flame, Vol. 63, 1986, pp. 381-413.

2. Yanenko, N. N., The Method of Fractional Steps, Springer-Verlag, New York, 1971.

3. Hirschfelder, J. O., Curtiss, C. F., and Bird, R. B., Molecular Theory of Gases and Liquids, John Wiley and Sons, Inc., New York, 1954.

4. Kuo, K. K., Principles of Combustion, John Wiley, New York, 1986.

5. Oran, E. S., and Boris, J. P., Numerical Simulation of Reactive Flows, Elsevier Publication, 1987.

6. MacCormack, R. W., and Baldwin, B. S., "A Numerical Method for Solving the Navier-Stokes Equations with Application to Shock Boundary Layer Interactions," AIAA Paper 75-1, 1975.

7. Brandon, D. M., Jr., "A New Single Step Implicit Integration Algorithm with A-Stability and Improved Accuracy," Simulation, 23, 17, 1974.

8. Radhakrishnan, K, and Pratt, D. T., "Fast Algorithm for Calculating Chemical Kinetics in Turbulent Reacting Flow," Combustion Science and Technology, Vol. 58, 1988, pp. 155-176.

9. Gardiner, W. C., Jr., Combustion Chemistry, Springer-Verlag, New York, 1984.

10. Peeters, J., and Mahnen, G., "Reaction mechanism and Rate Constants of Elementary Steps in Methane-Oxygen Flames," Fourteenth Symposium (International) on Combustion, 1973, pp. 133-146.

Table I
METHANE REACTION SCHEME

Arrhenius Rate Law: $AT^n \exp\left(-\frac{E}{RT}\right)$

Units are moles, cubic centimeters, second, Kelvin and calories/mole

	Reaction Scheme	A	n	E
1	CH4 + M = CH3 + H + M	.1000E+18	0.00	86000.0000
2	CH4 + O2 = CH3 + HO2	.7900E+14	0.00	56000.0000
3	CH4 + H = CH3 + H2	.2200E+05	3.00	8750.0000
4	CH4 + O = CH3 + HO	.1600E+07	2.36	7400.0000
5	CH4 + HO = CH3 + H2O	.1600E+07	2.10	2460.0000
6	CH2O + HO = CHO + H2O	.7530E+13	0.00	167.0000
7	CH2O + H = CHO + H2	.3310E+15	0.00	10500.0000
8	CH2O + M = CHO + H + M	.3310E+17	0.00	81000.0000
9	CH2O + O = CHO + HO	.1810E+14	0.00	3082.0000
10	CHO + HO = CO + H2O	.5000E+13	0.00	0.0000
11	CHO + M = H + CO + M	.1600E+15	0.00	14700.0000
12	CHO + H = CO + H2	.4000E+14	0.00	0.0000
13	CHO + O = HO + CO	.1000E+14	0.00	0.0000
14	CHO + O2 = HO2 + CO	.3000E+13	0.00	0.0000
15	CO + O + M = CO2 + M	.3200E+14	0.00	-4200.0000
16	CO + HO = CO2 + H	.1510E+08	1.30	-758.0000
17	CO + O2 = CO2 + O	.1600E+14	0.00	41000.0000
18	CH3 + O2 = CH3O + O	.7000E+13	0.00	25652.0000
19	CH3O + M = CH2O + H + M	.2400E+14	0.00	28812.0000
20	CH3O + H = CH2O + H2	.2000E+14	0.00	0.0000
21	CH3O + HO = CH2O + H2O	.1000E+14	0.00	0.0000
22	CH3O + O = CH2O + HO	.1000E+14	0.00	0.0000
23	CH3O + O2 = CH2O + HO2	.6300E+11	0.00	2600.0000
24	CH3 + O2 = CH2O + HO	.5200E+14	0.00	34574.0000
25	CH3 + O = CH2O + H	.6800E+14	0.00	0.0000
26	CH3 + HO = CH2O + H2	.7500E+13	0.00	0.0000
27	HO2 + CO = CO2 + HO	.5800E+14	0.00	22934.0000
28	H2 + O2 = HO + HO	.1700E+14	0.00	47780.0000
29	HO + H2 = H2O + H	.1170E+10	1.30	3626.0000
30	H + O2 = HO + O	.5130E+17	-0.82	16507.0000
31	O + H2 = HO + H	.1800E+11	1.00	8826.0000
32	H + O2 + M = HO2 + M	.2100E+19	-1.00	0.0000
33	H + O2 + O2 = O2 + HO2	.6700E+20	-1.42	0.0000
34	H + O2 + N2 = HO2 + N2	.6700E+20	-1.42	0.0000
35	HO + HO2 = H2O + O2	.5000E+14	0.00	1000.0000
36	H + HO2 = HO + HO	.2500E+15	0.00	1900.0000
37	O + HO2 = O2 + HO	.4800E+14	0.00	1000.0000
38	HO + HO = O + H2O	.6000E+09	1.30	0.0000
39	H2 + M = H + H + M	.2230E+13	0.50	92600.0000
40	O2 + M = O + O + M	.1850E+12	0.50	95560.0000
41	H + HO + M = H2O + M	.7500E+24	-2.60	0.0000
42	H + HO2 = H2 + O2	.2500E+14	0.00	700.0000

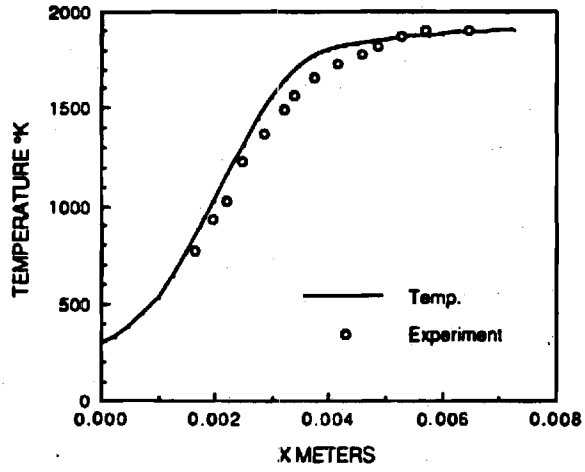

FIGURE 1. COMPARISON OF EXPERIMENTAL AND NUMERICALLY PREDICTED TEMPERATURE PROFILE VS. DISTANCE ABOVE BURNER SURFACE

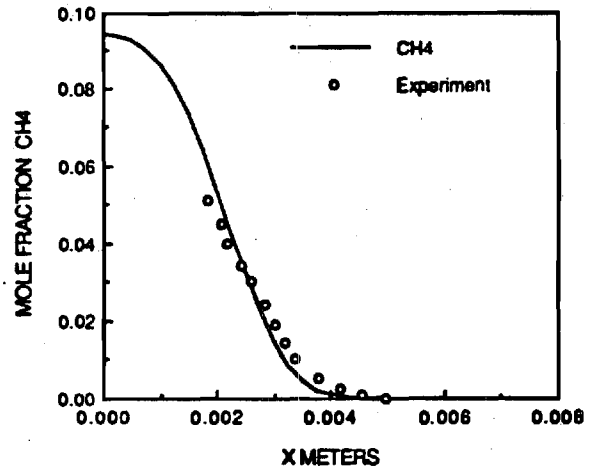

FIGURE 2. COMPARISON OF EXPERIMENTAL AND NUMERICALLY PREDICTED METHANE MOLE FRACTION PROFILE VS. DISTANCE ABOVE BURNER SURFACE

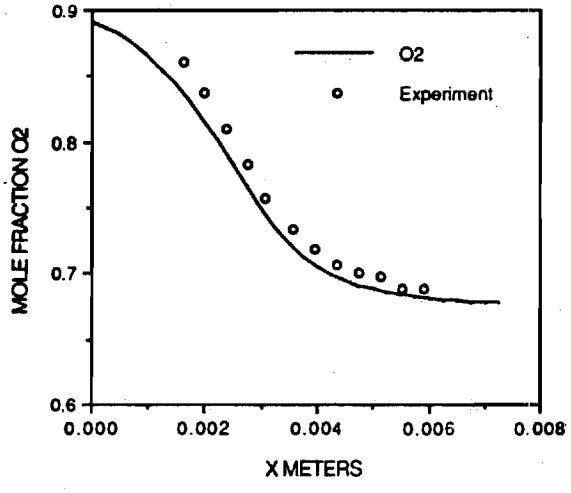

FIGURE 3. COMPARISON OF EXPERIMENTAL AND NUMERICALLY PREDICTED OXYGEN MOLE FRACTION PROFILE VS. DISTANCE ABOVE BURNER SURFACE

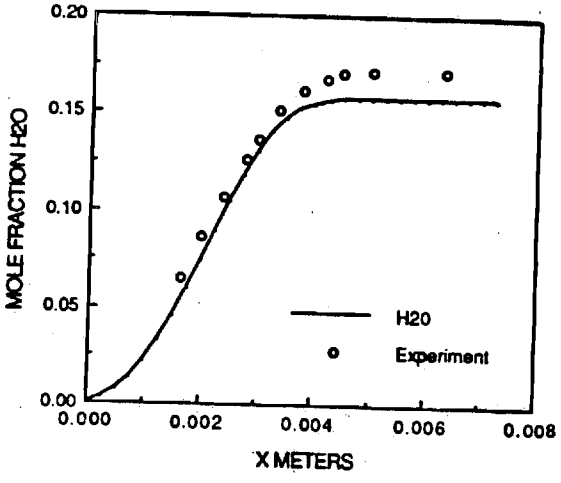

FIGURE 4. COMPARISON OF EXPERIMENTAL AND NUMERICALLY PREDICTED H2O MOLE FRACTION PROFILE VS. DISTANCE ABOVE BURNER SURFACE

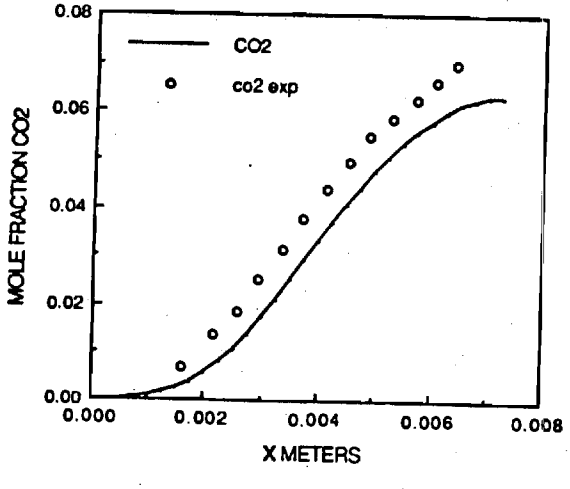

FIGURE 5. COMPARISON OF EXPERIMENTAL AND NUMERICALLY PREDICTED CO2 MOLE FRACTION PROFILE VS. DISTANCE ABOVE BURNER SURFACE

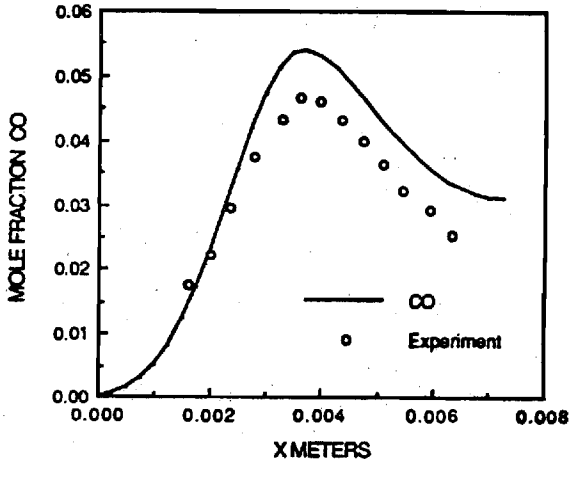

FIGURE 6. COMPARISON OF EXPERIMENTAL AND NUMERICALLY PREDICTED CO MOLE FRACTION PROFILE VS. DISTANCE ABOVE BURNER SURFACE

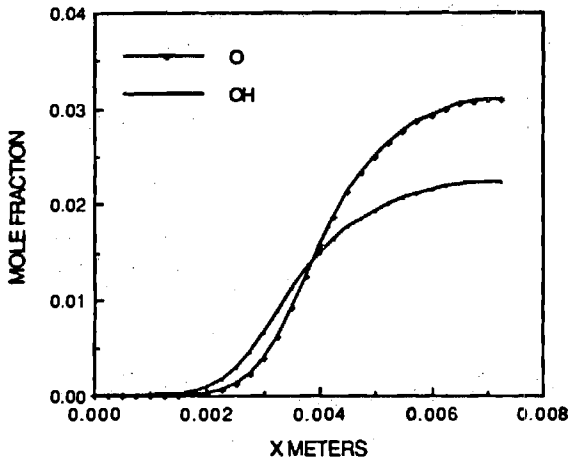

FIGURE 7. NUMERICALLY PREDICTED TRENDS OF OH AND O MOLE FRACTION PROFILES VS. DISTANCE ABOVE BURNER SURFACE

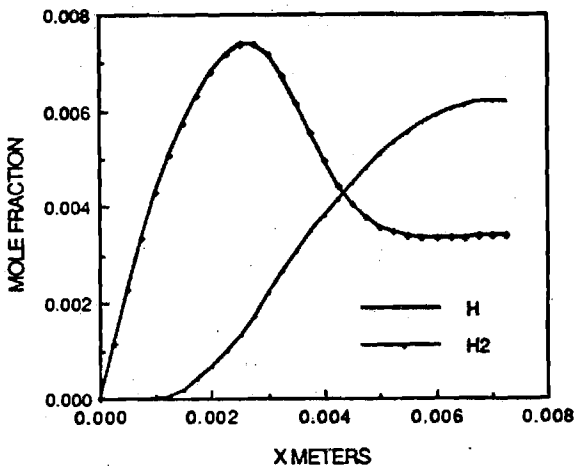

FIGURE 8. NUMERICALLY PREDICTED TRENDS OF H2 AND H MOLE FRACTION PROFILES VS. DISTANCE ABOVE BURNER SURFACE

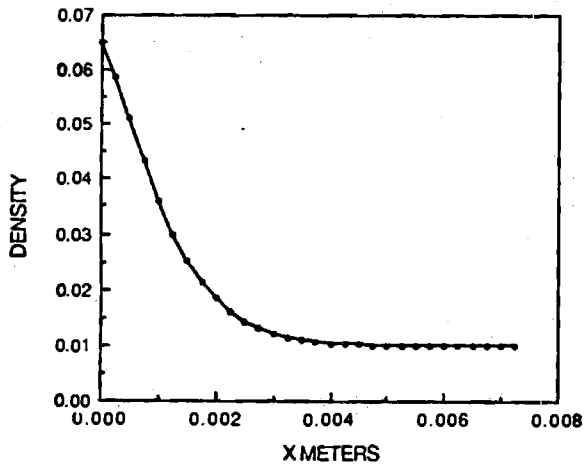

FIGURE 9. NUMERICALLY PREDICTED TREND OF DENSITY PROFILE VS. DISTANCE ABOVE BURNER SURFACE

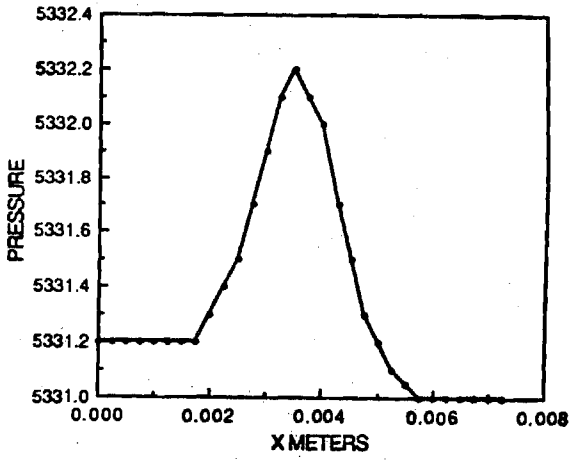

FIGURE 10. NUMERICALLY PREDICTED TREND OF PRESSURE PROFILE VS. DISTANCE ABOVE BURNER SURFACE

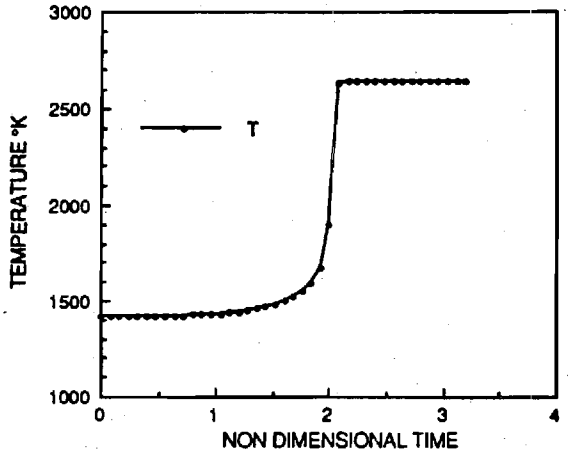

FIGURE 11. TEMPERATURE TIME HISTORY OF A VOLUME OF FLUID IN THE ABSENCE OF FLUID DYNAMIC EFFECTS

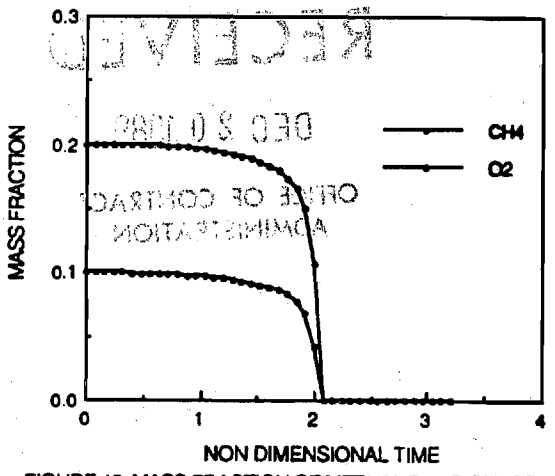

FIGURE 12. MASS FRACTION OF METHANE AND OXYGEN VS. NON DIMENSIONAL TIME

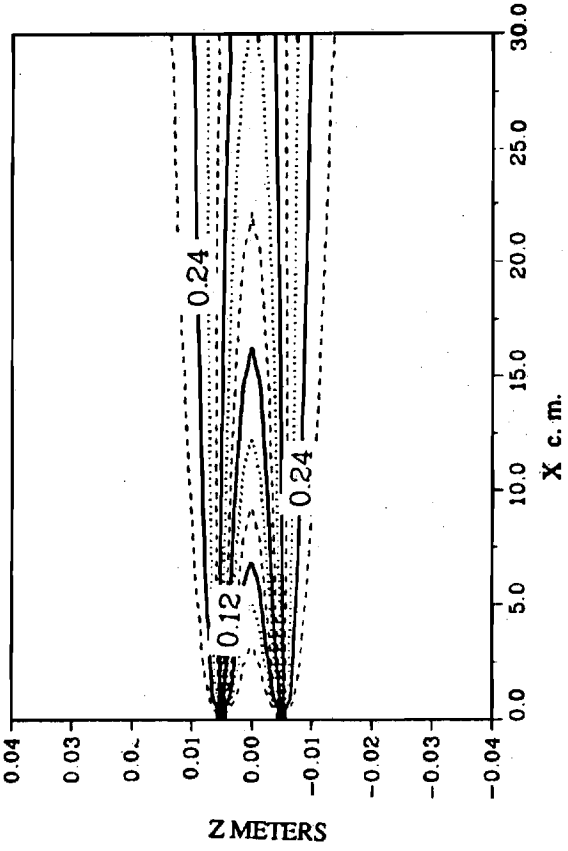

FIGURE. 13. CONSTANT OXYGEN DENSITY CONTOUR LINES ABOVE THE BURNER SURFACE

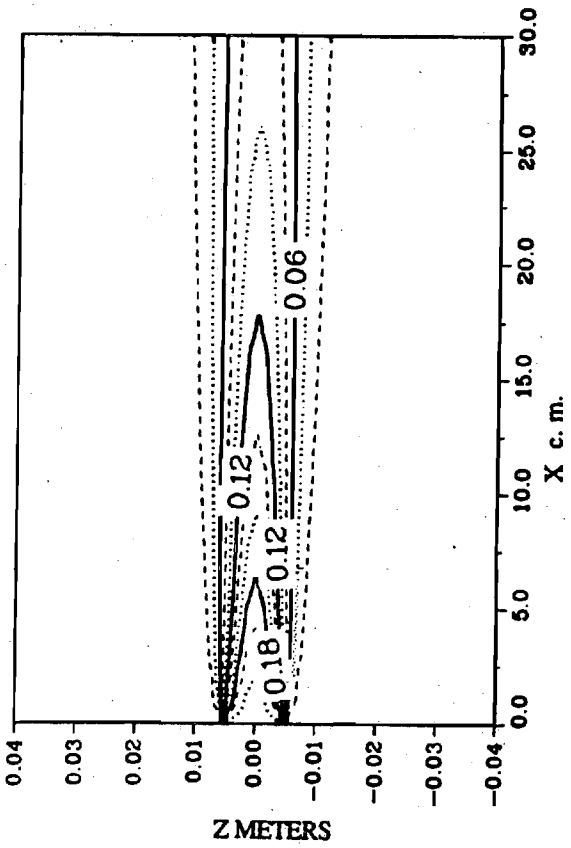

FIGURE. 14. CONSTANT METHANE DENSITY CONTOUR LINES ABOVE THE BURNER SURFACE